A Signal Processing Framework for Rapid Detection of Tree Defects via A Standoff Tree Radar System

Jiwei Qian(1), Yee Hui Lee(1), Daryl Lee(2), Mohamed Lokman Mohd Yusof(2), and Abdulkadir C. Yucel(1)
(1) The School of Electrical and Electronic Engineering, Nanyang Technological University, Singapore, 639798 (qian0069@e.ntu.edu.sg, eyhlee@ntu.edu.sg, acyucel@ntu.edu.sg)
(2) National Parks Board, Singapore, 259569 ({daryl_lee, mohamed_lokman_mohd_yusof}@nparks.gov.sg)

***Abstract*—This paper proposes a framework for processing the B-scans of tree trunks and revealing the presence of trees' internal defects (i.e., cavities and decays) from the signatures of their reflections. The framework uses the B-scans obtained by a standoff step frequency continuous wave radar system, moved in straight trajectories at a standoff distance facing the tree trunks' surfaces. In particular, the proposed framework first applies an antenna calibration to the raw B-scans to suppress the antenna's internal reflections. Then, it leverages a column-connection clustering (C3) algorithm to remove the signatures of the reflections from the trunk surface. Finally, it applies a Kaiser window to the Fourier-transformed A-scans of the processed B-scan to further increase the signal-to-noise ratio (SNR). The application of the proposed framework to measured (raw) B-scans shows that the proposed framework improves the SNR by more than 30 dB and reveals the signatures of the defects in the B-scans. The proposed framework can be used for many other standoff radar applications, such as through-the-wall imaging, defect/anomaly detection in concrete walls, in which the magnitude of the reflection from the main target is two/three orders smaller than the magnitude of the unwanted reflections from the surfaces or other objects.**

I. Introduction

Tree radar systems, leveraging ground penetrating radar principles, have been used to image the tree defects inside the tree trunks [1]. These systems collect the data while the systems are moved around the tree trunks' girths while in contact with their surfaces. Then the traditional signal processing and migration and/or full-waveform inversion algorithms are used to denoise the collected data (B-scan) and image the defects (such as cavities and decays) inside the tree trunks [2]. This process allows remarkably faster defect detection of trees compared to sonic tomography. However, such a process requires excessive setup time and manpower, hindering the tree radars' application to the large-scale structural health monitoring of trees in large urban forests. Recently, the notion of using a standoff radar system, moving on a straight trajectory facing one side of the trunk surface was proposed to detect tree defects and proven to be working via numerical studies [3]. However, when tested with real measurement data, the signal-to-noise ratio (SNR) of the B-scans obtained by the radar appears to be very low. Therefore, the signatures of the reflections from the tree defects are not distinguishable in B-scans.

This paper proposes a framework for processing the B-scans, improving their SNRs, and making the reflections from the tree defects distinguishable in the B-scans. The B-scans are obtained by a standoff step frequency continuous wave (SFCW) radar, while it is moved on a straight trajectory distanced from the tree trunk surface. The proposed framework first utilizes an antenna calibration to remove the antenna's internal reflections. Then it leverages a column-connection clustering (C3)-based zero-gating algorithm to eliminate the signatures of the reflections from the tree trunk surfaces. Finally, it applies a Kaiser window function to the Fourier-transformed A-scans to suppress the noise and clutter due to the high-frequency components. The proposed framework is applied to the raw B-scan of a *Pterocarpus indicus* (Angsana) tree trunk with a cavity. While more than 30 dB SNR improvement is achieved, the proposed framework output the B-scan with distinguishable reflection signatures of the tree defect.

II. Signal Processing Framework

The framework [Fig. 1(a)] first converts the collected frequency domain SFCW radar data to the time domain via inverse fast Fourier transform (IFFT), and then it stacks the obtained A-scans to generate a B-scan. Next, antenna calibration [4] is performed by deducting the signal measured without the object from each A-scan. This allows for the suppression of the antenna's internal reflections and revealing the signatures due to the reflections from the tree trunk surface and defects. To identify and remove the hyperbola due to the reflection from the trunk surface, the framework utilizes a C3-based zero-gating algorithm, implemented by three steps explained below.

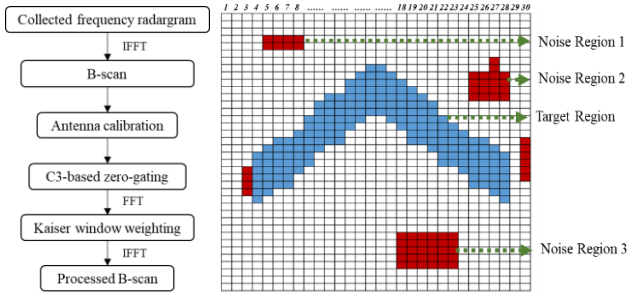

Figure 1. (a) The flow chart of the signal processing framework, and (b) an illustration of the C3-based zero-gating algorithm.

A. Binary image generation

The preprocessed B-scan is firstly converted to a binary image that only contains edge information detectable by edge detection operators. Then, an adaptive threshold selection strategy [5] is utilized to filter out the "edge" pixel with less intensity, in which way the maximum number of "edge" pixels

in the clutter region are reserved. An example of the generated binary images is shown in Fig. 1(b) where blocks with colors indicate retained "edge" pixels and each column corresponds to one A-scan.

B. C3 algorithm

C3 algorithm [5] is implemented to distinguish the target signal (blue) from noise (red) in Fig. 1(b). The fundamental unit in the algorithm is a segment that refers to a group of consecutive pixels in a column. Segments with less than a threshold value of pixels s are regarded as noise in which the value of s is determined by the noise level of the radar system. For Fig. 1(b), s is set to be 5, which classifies Noise Region 1, Noise Region 2, and the segment in column 3 successfully. Once the segments of signals in each column are obtained, the clustering is applied from the first column to the last, searching for spatially connected segments in the images where "connected" means two segments in adjacent columns have pixels from the same row. Additional prior information, such as the target cluster's hyperbolic shape, helps to filter out Noise Region 3 in the process, while only preserving the Target Region at the end.

C. Hyperbola fitting

To determine the row indices of the target cluster in traces that are not included, e.g., columns 1, 2, 3, 29, and 30, hyperbola fitting is performed by fitting segment position (x_k, y_k) in the clustered traces via solving $(x_k - d)^2/a^2 + y_k^2/b^2 = c$, where x_k and y_k are the column and row indices of the middle element of the segment, respectively. The parameters, a, b,c , and d are determined while minimizing the mean square error. Once regions of surface reflections are derived for all the traces, zero-gating is employed to remove the clutters.

Finally, a Kaiser window is utilized to weigh the frequency domain data of the zero-gated B-scan. By doing so, high-frequency components that contain noise and clutter are suppressed and the SNR of the B-scan is significantly improved.

III. Results and Discussions

An SFCW radar system [Fig. 2(a)], including an ultra-wideband dual-polarized Vivaldi antenna in a foam box, a Keysight vector network analyzer P5021A, and a laptop, is used for collecting frequency-domain data ranging from 0.5 GHz to 4 GHz with a total of 701 frequency points. An Angsana tree trunk sample with a diameter of 30 cm and a height of 50 cm is selected for the test. To mimic the cavity effect, a 6 cm-diameter hole is drilled off-center [Fig. 2(b)]. The SFCW radar is moved on a one-meter-long straight trajectory with a middle point positioned 10 cm away from the bark, while the antenna always faces the trunk. A total number of 51 A-scans are recorded to form the raw B-scan.

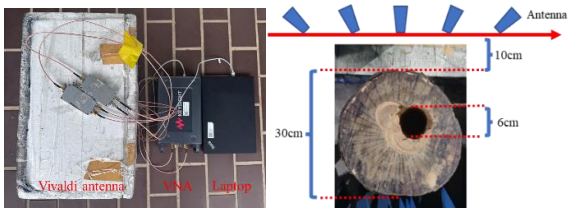

(a) (b)

Figure 2. (a)The SFCW radar system, and (b) the Angsana trunk sample

Fig. 3 illustrates the B-scans obtained at different processing stages. Specifically, the antenna's internal reflection is effectively removed through antenna calibration [Fig. 3(b)]. After applying the C3-based zero-gating algorithm, the clutter due to the reflection from the bark is completely removed [Fig. 3(c)] so that the scattering from the trunk interior is better revealed. After applying a proper Kaiser window, the cavity reflection, an internal hyperbolic curve, become more distinguishable from the noise. Since the cavity is located off-center, the apex of the corresponding hyperbolic curve shifts to the right side of the B-scan in Fig. 3(d). Additionally, the SNR of B-scans of raw data is improved from -13.9 dB to 3.6 dB, 15.0 dB and 16.4 dB after applying antenna calibration, C3-based zero-gating, and Kaiser window weighting, respectively. In short, the framework improves the SNR by more than 30 dB.

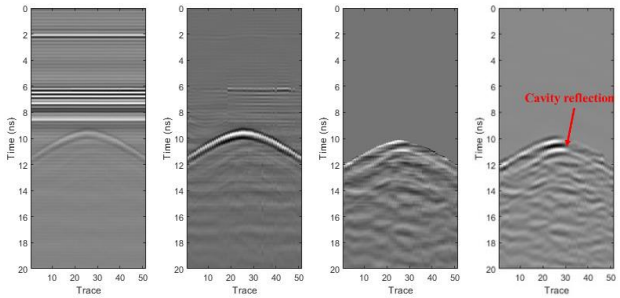

(a) (b) (c) (d)

Figure 3. B-scans at different processing stages: (a) raw data, (b) antenna calibration, (c) C3-based zero-gating, and (d) Kaiser window weighting.

IV. Conclusion

This study proposes a signal processing framework to detect the signatures of the tree defects in B-scans obtained via a standoff SFCW radar. The framework improves the SNR by more than 30 dB and makes the defects' signatures distinguishable in B-scans.

Acknowledgment

This work was supported by the Ministry of National Development under the Cities of Tomorrow (CoT) R&D Programme with Award No. COT-V4-2020-6.

References

[1] S. Gokkan and C. Ozdemir, "Tree-interior radar (TIR) imaging using matching pursuit algorithm and comparison to other TIR focusing techniques," *Digital Signal Processing*, vol. 118, pp.1-12, 2021.

[2] I. Giannakis, F. Tosti, L. Lantini, and A. M. Alani, "Health monitoring of tree trunks using ground penetrating radar," *IEEE Trans. Geosci. Remote Sens*, vol. 57, (10), pp.8317-8326, 2019.

[3] Q. Dai, B. Wen, Y. H. Lee, A. C. Yucel, G. Ow, and M. L. M. Yusof, "A deep learning-based methodology for rapidly detecting the defects inside tree trunks via GPR," in *Proc. USNC-CNC-URSI North America Radio Science Meeting*, Montreal, QC, Canada, Jul. 2020, pp.1-2.

[4] S. Lambot, E. C. Slob, I. Bosch, B. Stockbroeckx, and M. Vanclooster, "Modeling of ground-penetrating radar for accurate characterization of subsurface electric properties," *IEEE Trans. Geosci. Remote Sens*, vol. 42, (11), pp.2555-2568, 2004.

[5] Q. Dou, L. Wei, D. R. Magee, and A. G. Cohn, "Real-time hyperbola recognition and fitting in GPR data," *IEEE Trans. Geosci. Remote Sens*, vol. 55, (1), pp.51-62, 2017.